Identification of Two New Electronic Transitions of TaF using Intracavity Laser Spectroscopy

Kristin N. Bales,[1] Jack C. Harms,[1] Leah C. O'Brien,[2] and James J. O'Brien[1]

[1]*Department of Chemistry and Biochemistry & Center for Nanoscience, University of Missouri – St. Louis, Saint Louis, MO 63121, USA*

[2]*Department of Chemistry, Southern Illinois University Edwardsville, Edwardsville, IL 62026, USA*

Abstract

Several bands in two new electronic transitions of TaF have been recorded in high resolution using intracavity laser absorption spectroscopy (ILS). The (1,0), (0,0), and (0,1) bands of the [16.0]0^+ – $X\,^3\Sigma^-(0^+)$ transition and the (2,1), (1,0), (0,0), (0,1), and (1,2) bands of the [16.3]1 – $X\,^3\Sigma^-(0^+)$ transition were observed. TaF was produced in the plasma discharge of a tantalum-lined copper hollow cathode with Ar [1 torr] as a sputter gas and trace of SF_6 as a fluoride source. Trace H_2 [1 %] also was used as it was found to increase the intensity of the observed transitions. The transitions were analyzed using PGOPHER, and the obtained molecular parameters are presented and compared with a previous work.

Introduction

The electronic structure of tantalum fluoride has not been studied comprehensively, with the only published work on TaF provided by Ng *et al*. in 2017.[1] Laser Induced Fluorescence (LIF) in a molecular beam was used to examine 22 vibrational bands in seven electronic transitions in the visible region from 18,000 – 23,000 cm^{-1}. Molecular constants were determined for seven upper states, [18.6]0, [19.8]0, 19.9]0, [22.1]0, [22.9]0, and [18.1]1, and two lower states, $X\,^3\Sigma^-(0^+)$ and $A\,^3\Phi_2$. A computational analysis at the MRCISD+Q (internally contracted multi-reference configuration interaction with singles and doubles and Davidson's cluster correction) level of theory of several low-lying Λ-S states also was presented as part of the work. Potential energy curves for these states were shown as well as term energies, equilibrium bond lengths, and vibrational and rotational constants. Additionally, transition dipole moments were presented indicating the strength of various electronic transitions.

In this work, we observed and analyzed eight additional bands belonging to two new electronic transitions of TaF, specifically the (1,0), (0,0), and (0,1) vibrational bands of the $[16.0]0^+ - X\,^3\Sigma^-(0^+)$ transition and the (2,1), (1,0), (0,0), (0,1), and (1,2) bands of the $[16.3]1 - X\,^3\Sigma^-(0^+)$ transition. The transitions were observed using intracavity laser spectroscopy (ILS), and the measured line positions were fit using PGOPHER[2] to obtain molecular constants, which are presented here with comparisons to the previous work by Ng *et al*.[1] These transitions are illustrated, in addition to those observed previously, in Figure 1. While our determined molecular constants agree with those calculated, the observed $[16.0]0^+ - X\,0^+$ transition was predicted to have a very low transition dipole moment[1] and was expected to be weak.

Experimental Method

The spectra were collected in the visible region using intracavity laser absorption spectroscopy (ILS). The ILS system, incorporating a dye laser, has been described in detail previously.[3] Briefly, TaF molecules were produced in the plasma discharge of a 50 mm long tantalum-lined copper hollow cathode as an RF current of 0.30 – 0.60 A was applied.

Approximately 1 torr of Ar was used as sputter gas, and a trace of SF_6 [0.5%] used as a reagent gas supplied the fluoride. It was found that including a trace amount of H_2 [1%] in the gas mixture increased the intensity of the observed transitions, though the exact cause of this increase is not known. The laser dyes used, DCM and R6G, allowed data collection over the range of 14,500 – 17,150 cm^{-1}. Generation times of 50 – 200 μs were used, giving an effective pathlength of 0.74 - 2.96 km for the 50 mm hollow cathode in a 1.01 m resonator cavity. As previously described,[3] each plasma spectrum was divided by a background spectrum taken in the absence of the plasma and measured soon after the plasma spectrum was recorded at the same monochromator location. An I_2 spectrum from a heated extra-cavity cell was recorded immediately following each TaF spectrum to allow calibration using reference data from Salami and Ross.[4] Isolated lines are estimated to have an accuracy of ±0.005 cm^{-1}.

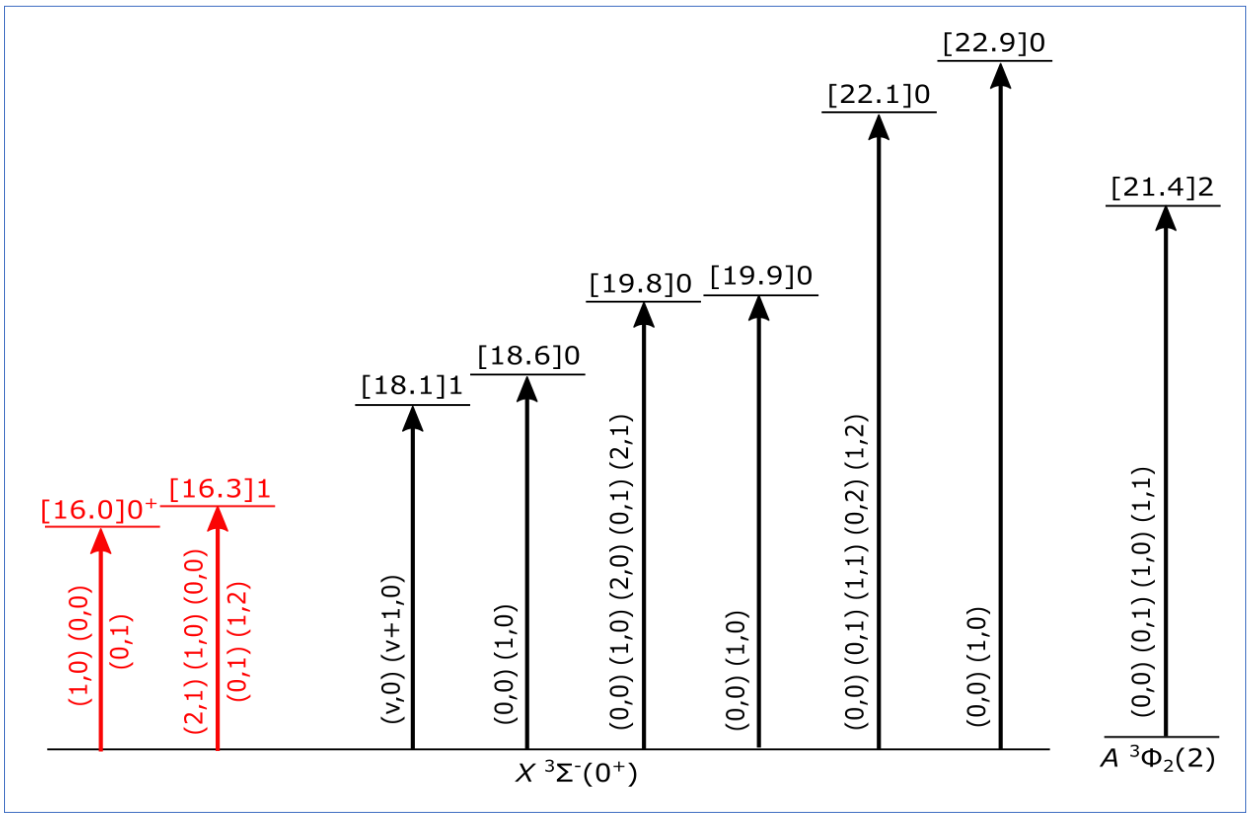

Figure 1. Illustration of observed transitions of TaF. The two new electronic transitions observed in this work are shown on the left (in red), while the 7 known transitions[1] are on the right (in black).

Results and Discussion

The work published by Ng *et al.*[1] included a computational analysis that predicted several observable transitions in the visible region accessible by the ILS system when used in conjunction with the R6G and DCM laser dyes. In this work, eight bands were observed and recorded at rotational resolution between 14,850 – 16,950 cm^{-1}. These were identified as the (1,0), (0,0), and (0,1) vibrational bands of the $[16.0]0^+ - X\,^3\Sigma^-(0^+)$ transition and the (2,1), (1,0), (0,0), (0,1), and (1,2) bands of the $[16.3]1 - X\,^3\Sigma^-(0^+)$ transition.

To obtain the vibrational assignments the eight observed bands first were sorted into two vibrational progressions. Secure vibrational assignments were made based on the known vibrational constants of the $X\,^3\Sigma^-(0^+)$ state. For each vibrational progression, two bands were separated by 697 cm^{-1}, consistent with the $\Delta G_{1/2}$ value reported by Ng *et al.*[1] for the $X\,^3\Sigma^-(0^+)$ state. The four bands were correspondingly assigned as (0,0) and (0,1) bands of these two transitions, with the two (0,0) bandheads observed near 16,033 cm^{-1} and 16,327 cm^{-1}. Further vibrational assignments were thus straightforward: two bands were observed ~600 cm^{-1} higher in energy than the (0,0) bands, consistent with the vibrational frequencies predicted for the excited states of TaF,[1] and these bands were assigned as (1,0) bands; slightly weaker bands were also observed ~95 cm^{-1} to the red of the (1,0) and (0,1) bands of the 16,327 cm^{-1} system, and were assigned as (2,1) and (1,2) bands, respectively. Ta has only one major stable isotope (^{181}Ta, 99.988% abundant), and thus isotope shifts are not available to further confirm the vibrational assignments.

Each band of the 16,033 cm^{-1} system consisted of only two branches: a single P- and a single R-branch as illustrated in Figure 2. Combination differences between these branches in the all three observed bands were in agreement with the Δ_2F'' levels from Ng *et al.*[1] for v=0 and 1 of the $X\,^3\Sigma^-(0^+)$ state, confirming the rotational assignment and the initial vibrational assignment. The lack of a Q-branch indicates that the excited state must be $\Omega=0^+$ in character, so the band system has been assigned as the $[16.0]0^+ - X\,^3\Sigma^-(0^+)$ transition of TaF.

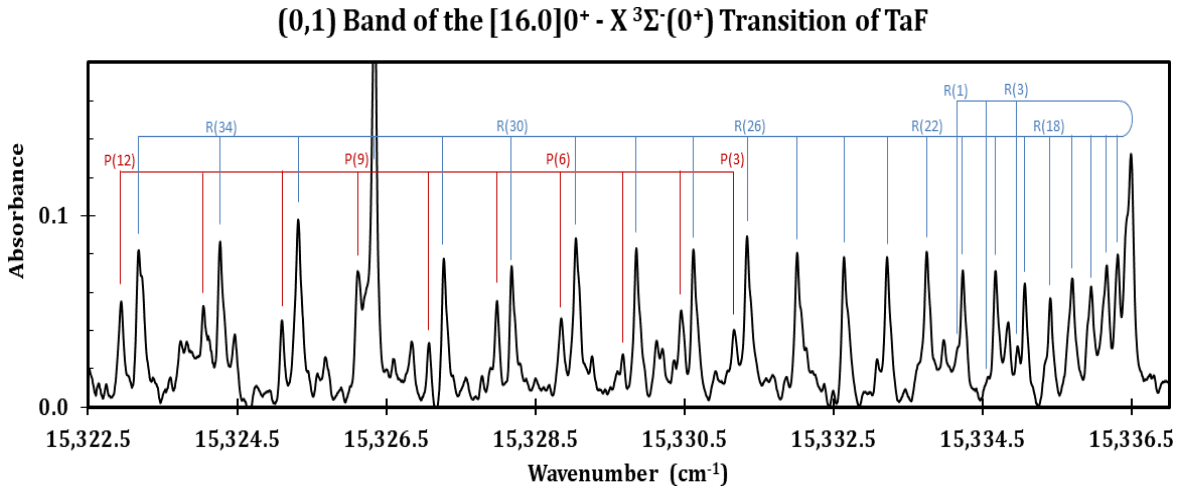

Figure 2. Bandhead portion of the (0,1) band of the [16.0]0^+ – $X\,^3\Sigma^-(0^+)$ transition of TaF, showing P- and R-branches with no Q branch indicating a $\Delta\Omega=0$ electronic transition. Unlabeled peaks in this spectrum and in Figure 3 are not considered to be noise as they are reproducible. Additional lines may be high-J lines of other TaF transitions due to the energetic molecular source, or due to transitions of other species such as TaS formed in the chamber stemming from the use of SF_6 as a reagent gas.

The bands of the 16,327 cm^{-1} system consisted of a P-, a Q-, and an R-branch, as illustrated in Figure 3. Again, combination differences between the P- and R-branches were in agreement with the Δ_2F'' levels from Ng *et al.*[1] for v=0, 1 and 2 of the $X\,^3\Sigma^-(0^+)$ state, confirming the rotational assignment and the initial vibrational assignment. The strong Q-branch indicates that the transition is $\Delta\Omega=+1$, so the band system has been assigned as the [16.3]1 – $X\,^3\Sigma^-(0^+)$ transition of TaF.

The rotational branches were fit to a Hund's Case (c) Hamiltonian using PGOPHER.[2] Line positions from five transitions observed by Ng *et al.*[1] that also originate in the $X\,^3\Sigma^-(0^+)$ ground state were included in the fit to minimize correlation among the fitted constants. In total, 1238 observations were fit to 50 parameters. Twenty-six of these parameters were related to the $X\,^3\Sigma^-(0^+)$, [16.0]0^+, and [16.3]1 states, with the remaining parameters pertaining to the previously observed excited states. The 26 parameters determined for the $X\,^3\Sigma^-(0^+)$, [16.0]0^+, and [16.3]1 states are given in Table 1. A comparison of the experimental spectrum to the PGOPHER[2] simulation of the (0,1) band of the [16.3]1 – $X\,^3\Sigma^-(0^+)$ transition is provided in Figure 3.

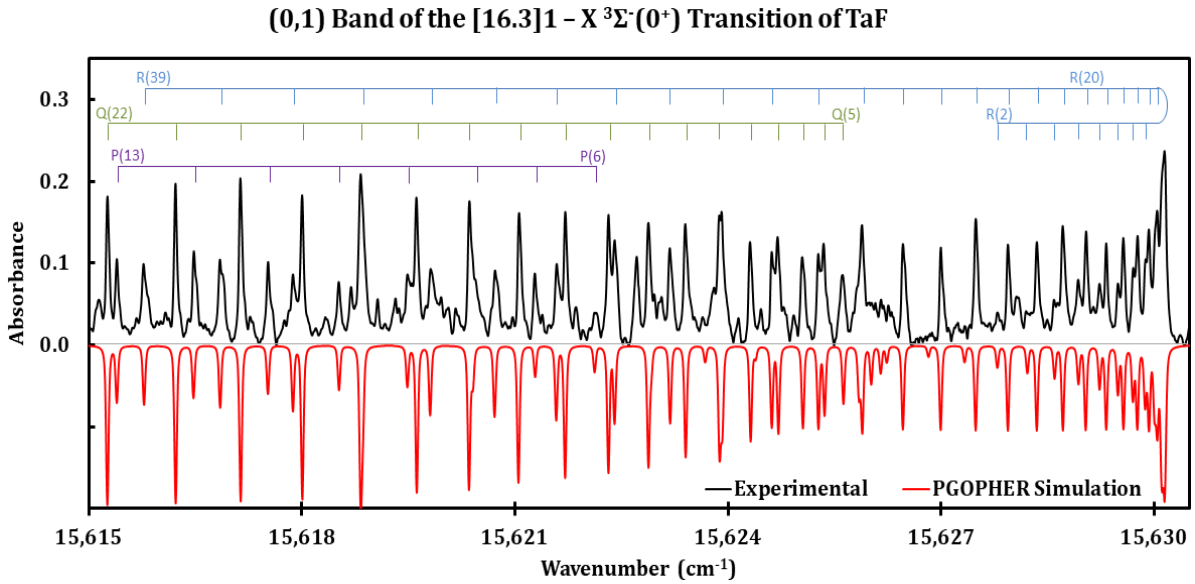

Figure 3. Bandhead portion of the (0,1) band of the [16.3]1 – $X\,^3\Sigma^-(0^+)$ transition of TaF with the experimental spectrum in black (top) and the PGOPHER simulation in red (bottom). For the simulation, the Gaussian and Lorentzian linewidths were set to 0.03 cm^{-1} with T= 500 K. The strong Q-branch is indicative of a $\Delta\Omega=\pm1$ electronic transition.

Table 1. TaF molecular constants (in cm^{-1}) for the $X\,^3\Sigma^-(0^+)$, $[16.0]0^+$, and [16.3]1 states from this work are shown in **bold**, with 1 σ error shown in parenthesis. Previous literature values[1] are provided in *italics*.

State	Vibrational Level	T_v	B_v	D_v x 10^6	q_v x 10^6
$X\,^3\Sigma^-(0^+)$	v=0	**0**[a]	**0.296036(10)**	**0.2121(48)**	**-**
		0	*0.2961(1)*[b]	*0.2961(1)*[b]	-
	v=1	**697.0511(10)**	**0.294286(10)**	**0.2132(48)**	**-**
		697.02(1)[b]	*0.2943(1)*[b]	*0.2943(1)*[b]	-
	v=2	**1388.0977(26)**	**0.292518(14)**	**0.2076(91)**	**-**
		1388.11(1)[b]	*0.2926(1)*[b]	*0.2926(1)*[b]	-
$[16.0]0^+$	v=0	**16030.1291(10)**	**0.2709921(96)**	**0.2291(44)**	**-**
	v=1	**16613.0512(16)**	**0.269303(10)**	**0.2249(49)**	**-**
[16.3]1	v=0	**16323.22755(100)**	**0.273011(11)**	**0.1883(55)**	**1.0158(13)**
	v=1	**16919.0076(15)**	**0.271290(11)**	**0.3208(66)**	**0.9883(13)**
	v=2	**17509.0258(36)**	**0.269809(22)**	**0.240(27)**	**0.9808(49)**

[a]Held fixed in fit
[b]Ref. 1.

Equilibrium rotational constants (B_e) and bond lengths (R_e) were calculated for the [16.0]0^+ and [16.3]1 states using the determined rotational constants, B_v. Additionally, the equilibrium term energy (T_e), vibrational constant (ω_e), and anharmonicity constant ($\omega_e x_e$) were calculated for the [16.3]1 state, and $\Delta G_{1/2}$ was calculated for the [16.0]0^+ state. These determined equilibrium constants are given in Table 2.

Table 2. Equilibrium constants for the $X\,^3\Sigma^-(0^+)$, [16.0]0^+, and [16.3]1 states of TaF are shown in **bold.** Values predicted or observed by Ng *et al.*[1] are shown in *italics*.

State	B_e (cm^{-1})	r_e (Å)	T_e (cm^{-1})	ω_e (cm^{-1})	$\omega_e\chi_e$ (cm^{-1})	$\Delta G_{1/2}$ (cm^{-1})
X $^3\Sigma^-(0^+)$	**0.2969**	**1.817**	**0**[a]	**703.1**	**3.00**	**697.1**
{1}0^+	*0.2989*[b]	*1.811*[b]	*0*[b]	*701.3*[b]	*1.69*[b]	*697.9*[c]
[16.0]0^+	**0.2718**	**1.899**	**16030**[d]	**-**	**-**	**582.9**
{7}0^+	*0.2694*[b]	*1.908*[b]	*16659*[b]	*573.2*[b]	*1.61*[b]	*570.0*[c]
[16.3]1	**0.2738**	**1.892**	**16374**	**601.5**	**2.88**	**595.8**
{11}1	*0.2703*[b]	*1.905*[b]	*16874*[b]	*599.7*[b]	*2.12*[b]	*595.5*[c]

[a] *T_v values from Table 1 were adjusted to compensate for the zero-point energy of the ground state.*
[b] *Predicted value from Ref. 1.*
[c] *From predicted ω_e and $\omega_e x_e$ values.*
[d] *T_{00} value.*

The experimental molecular constants were compared to those the computational predictions.[1] Based on symmetry (Ω value) and excited state molecular constants, the new experimentally observed excited electronic states best correlate to the [7]0^+ and [11]1 states from the computation. Neither of these excited states were used for the 7 previously identified electronic states.[1] For comparison, the molecular constants from the computational work for these states are included in Table 2. In general, the agreement between the experimentally observed states and these predicted states is quite good.

Interestingly, the [11]1 – $X\,^3\Sigma^-(0^+)$ transition was predicted to have one of the largest transition dipole moments of any TaF transition at 0.476,[1] where the [11]1 state is primarily $^3\Pi_1$ in character and thus this transition is fully allowed. The observed transition to the [7]0^+ – $X\,^3\Sigma^-(0^+)$ transition was calculated to have a very low transition dipole moment of 0.006, and, therefore, would not be expected to be readily observable.

However, this excited state includes considerable $^3\Pi_{0+}$ character, and the transition dipole is perhaps undervalued due to the non-orthogonal SOC method in MOLCAS.[5] Spectral lines corresponding to this transition were quite strong considering the low transition dipole moment predicted; however, the difference may help to explain why fewer bands of the [16.0]0^+ – $X\,^3\Sigma^-(0^+)$ transition were observed compared to the other transition.

Conclusions

Eight vibrational bands of two new electronic transitions of TaF have been recorded using intracavity laser absorption spectroscopy and were rotationally analyzed. Molecular constants for the [16.0]0^+ and [16.3]1 states are presented. Molecular constants for the $X\,^3\Sigma^-(0^+)$ ground state have improved the accuracy of those given previously. Transition energies for the excited states were found to be roughly 500 cm^{-1} lower than those predicted,[1] and other spectroscopic parameters agreed well with predictions. The most notable difference from the computational study was in the observed strength of the [16.0]0^+ transition given the very low predicted transition dipole moment.

Supplementary Materials

Three files involved in the PGOPHER fits are included in the Supplementary Materials and are sufficient to reproduce the analysis: the main PGOPGHER file (TaF.pgo); an overlay file (TaF.ovr) containing the concatenated ILS spectra; and the results of the fit (TaF.lin) which include line positions, fit residuals, and fitted constants with correlation matrix.

Acknowledgements

Funding for this work was provided by the National Science Foundation, Grant Nos. CHE-1566454 (JOB) and CHE-1566442 (LOB). J. C. Harms would also like to acknowledge the UMSL Graduate School for providing additional funding for this project through a Dissertation Fellowship.

References

1. K. F. Ng, W. Zou, W. Liu, A.S.-C. Cheung. Electronic transitions of tantalum monofluoride. *J. Chem. Phys.*, **146**, 094308-1 – 094308-6 (2017).

2. PGOPHER, A Program for Simulating Rotational, Vibrational and Electronic Spectra, C. M. Western, *JQSRT*, **186,** 221-242 (2016) doi:10.1016/j.jqsrt.2016.04.010.

3. J. C. Harms, L. C. O'Brien, J. J. O'Brien. The spin-forbidden $a\ ^4\Sigma^-$-$X\ ^2\Pi_{1/2}$ transition of GeH detected in absorption using intracavity laser spectroscopy. *J. Chem Phys.*, **148**, 204306-1 – 204306-7 (2018).

4. H. Salami and A. J. Ross. A molecular iodine atlas in ascii format. *J. Mol. Spec.*, **223**, 157 – 159 (2005).

5. Wenli Zou, personal communication (2018).